UDC 539.4

Cryogenic Fracture Behavior of Metastable Austenitic Stainless Steel in a High Magnetic Field

Y. Shindo, F. Narita, M. Suzuki, and I. Shindo

Department of Materials Processing, Graduate School of Engineering, Tohoku University, Sendai, Japan

УДК 539.4

Особенности разрушения метастабильной аустенитной нержавеющей стали при криогенных температурах в высокоинтенсивных магнитных полях

Я. Шиндо, Ф. Нарита, М. Сузуки, И. Шиндо

Отделение обработки материалов, Университет Тохоку, Сендай, Япония

Исследуется влияние магнитного поля на закономерности разрушения метастабильной аустенитной нержавеющей стали при криогенных температурах. При испытании компактных образцов на растяжение в среде жидкого гелия при температуре 4 К при наличии и отсутствии магнитного поля получены экспериментальные значения упругопластической вязкости разрушения и проанализировано влияние магнитного поля на эти параметры. С помощью магнитного метода выполнен количественный фазовый анализ. Поверхности разрушения исследовались на сканирующем микроскопе с целью оценки корреляции полученных параметров разрушения.

Ключевые слова: механика разрушения, растяжение компактных образцов, аустенитная нержавеющая сталь, вязкость разрушения, температура жидкого гелия, магнитное поле, сврхпроводящие электромагниты для ядерного синтеза.

Introduction. Metastable austenitic stainless steels are used in the superconducting magnet structures. In this application the alloys sustain high stresses in high magnetic fields at liquid helium temperature (4 K). This necessitates complete characterization of the fracture and deformation behavior of these alloys at the anticipated operating conditions. These metastable austenitic stainless steels can undergo strain-induced martensitic transformation at cryogenic temperatures [1]. Also, magnetic fields tend to raise the martensitic transformation temperature and to increase the amount of transformation in ferrous alloys.

Fukushima et al. [2] performed the fracture tests on 304 stainless steel using compact tension (CT) specimens precracked at 77 K, and suggested that there may be a significant decrease in the fracture toughness at 4 K in a 9 T magnetic field. Murase et al. [3] also observed that an 8 T magnetic field decreased the 4 K fracture toughness of 304 CT specimens precracked at 77 K. On the other hand, Chan et al. [1] conducted the fracture tests using CT specimens precracked at room

temperature (RT) and found that an increase in the fracture toughness of 304 stainless steel tested at 4 K in an 8 T magnetic field was observed relative to the fracture toughness of stainless steel tested in 0 T. They concluded that this improvement is expected as a result of magnetostatic effects and transformation strain differences due to the excess martensite formed within the magnetic field, and the increase in strain hardening rates. The direction of fracture toughness change is influenced both by the stability of the alloys and by the specimen preparation conditions, such as precracking temperature. Further, Chan et al. [4] discussed the fracture behavior of CT specimens made from austenitic stainless steels of differing stability in a 4 K, 8 T magnetic field environment. The least stable alloy showed a large reduction in the 4 K fracture toughness with an 8 T magnetic field, and the amount of fracture toughness reduction with an 8 T magnetic field decreased as the stability of the specimens increased. They found that this difference in fracture behavior is attributed to the enhancement of martensitic transformation about the crack tip during the fracture process in a magnetic field.

Recently, Yamaguchi et al. [5] studied the effect of magnetic field on the cryogenic fracture properties in a ferromagnetic austenitic alloy using small punch (SP) and notch tensile specimens. The 4 K fracture properties of alloy 908 were not changed significantly by magnetic field. Shindo et al. [6] also examined the effect of magnetic field on the fracture properties of SUS 304 and 316 at 4 K. SUS 304 showed a decrease in the measured fracture toughness at 4 K with the application of magnetic field. However, the magnetic field effect was not large enough to affect mechanical design for SUS 316. They concluded that the magnitude of change in 4 K fracture toughness with the application of magnetic field is a function of the stability of the alloy.

In this paper, we investigate the effect of magnetic field on the cryogenic fracture properties of metastable austenitic stainless steel SUS 304. Elastic-plastic fracture toughness (J_{Ic}) tests were performed on side-grooved CT specimens at 4 K with and without a magnetic field, following JIS Z 2284 [7]. The specimens were fatigue precracked at RT and 77 K. *J*-resistance (*J–R*) curves were generated by the single specimen unloading-compliance test technique, and the magnetic field dependence of the cryogenic fracture toughness was discussed. The volume fraction of martensite was also determined using magnetic method, and the fracture surfaces were examined using scanning electron microscopy (SEM) to correlate with fracture characteristics.

Experimental Procedure. The compositions of the commercial SUS 304 used in this work are listed in Table 1. SUS 304 is metastable with respect to austenitic-to-martensitic transformation and undergo a phase transition from an fcc structure to a more stable bcc martensite on deformation at low temperatures.

T a b l e 1

Chemical Compositions of SUS304 Stainless Steel (wt.%)

C	Si	Mn	P	S	Ni	Cr
0.06	0.47	0.89	0.028	0.001	8.54	18.28

The CT specimen was 5 mm thick (B) and 25 mm wide (W), i.e., 0.2TCT [8]. The specimens were fatigue precracked at RT and 77 K with final stress intensity factor range of 30 MPa $\cdot$ m$^{1/2}$. The precracking was continued to the original-crack-length-to-width ratio $a_0/W = 0.6$. After precracking, side-grooves were machined on all specimens to a net thickness (B_N) reduction of 20%.

A 30 kN axial loading capacity servo-hydraulic testing machine was employed. A cryocooler-cooled superconducting magnet, 10 T (tesla) capacity, with a 100 mm diameter working bore was also used to create a static uniform magnetic field of magnetic induction $B_0 = 6$ T. Low temperature environment was archived by immersing the load frame, specimen, and clip gage in liquid helium (4 K). Before J_{Ic} testing, tensile tests were conducted on the SUS304 specimens in accordance with ISO 19819 [9], and Youngs modulus E, Poissons ratio ν, 0.2% proof stress $\sigma_{0.2}$, ultimate tensile strength σ_u, and fracture strain ε_f were measured. The ferrite content was also measured using a conventional ferrite tester equipment (Ferrite scope). The 4 K J_{Ic} testing was then done. The specimens were loaded at a constant clip-gage displacement rate of 0.12 mm/min. The single-specimen unloading compliance method described in JIS Z 2284 was used to monitor the crack growth and obtain the fracture toughness parameters. The specimen was periodically unloaded by approximately 10% and then reloaded to a higher J level. The slope of the unloading curve was measured and related to crack length (a) by compliance, and the crack length was used to obtain the crack extension increment ($\Delta a = a - a_0$). Value of J was calculated from the load–displacement record and specimen dimensions.

After J_{Ic} testing, the final physical crack length a_p, the distance from the load line to the final crack front, was measured with a digital microscope. The dimension ap was taken as the average of nine physical measurements a_{pi} ($i = 1$–9) taken at nine equally spaced points centered about the specimen centerline and extending to $0.005W$ from the root of the side groove specimen. The two near-surface measurements were average into one value and the result was used along with the remaining seven crack length measurements. Similarly, the final value of physical crack extension Δa_p was taken as the average of nine similar measurements Δa_{pi} ($i = 1$–9) between the original crack front and the end of stable crack growth.

Results and Discussion. Two typical stress–strain curves of the SUS304 tensile specimens at 4 K are shown in Fig. 1. Serrations are formed by repeated bursts of unstable plastic flaw and arrests. Table 2 shows the Youngs modulus E, Poissons ratio ν, 0.2% proof stress $\sigma_{0.2}$, ultimate tensile strength σ_u, and fracture strain ε_f with and without magnetic field. It is shown that magnetic field has negligible effect on the tensile properties. Table 3 lists the measured ferrite contents at 4 K. Also listed are the ferrite contents at RT for comparison. As the strain increases, the ferrite content increases. Also, the decrease in the temperature results in an increase in ferrite content. At 4 K, we observed almost 18% increase in ferrite content in the magnetic field of 6 T under strain at fracture. Since the increase in martensite content is correlated with the increase in the ferrite content, the martensite content increases under strain at fracture as the magnetic field increases at 4 K.

T a b l e 2

Tensile Properties of SUS304 Stainless Steel at 4 K

B_0, T	E, GPa	ν	$\sigma_{0.2}$, MPa	σ_u, MPa	ε_f
0	192	0.30	354	1691	0.35
6	192	0.29	340	1706	0.33

T a b l e 3

Variation of Ferrite Content with Applied Strain

Temperature (K)	Magnetic induction B_0, T	Strain	Ferrite content (%)
RT	0	0.002	1.33
		0.200	1.60
		0.690	48.70
4	0	0.08	3.70
		0.35	75.00
	6	0.08	4.68
		0.33	88.20
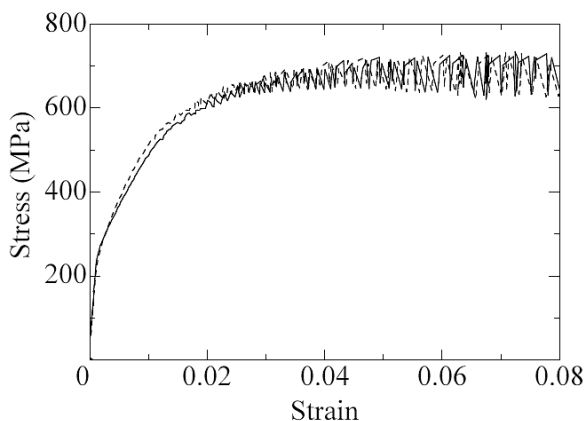
Fig. 1. Stress–strain curves for SUS304 tensile specimens at 4 K. (Here and Figs. 2–5: solid lines – with the magnetic field of 6 T and dashed lines – without the magnetic field.)

Figure 2 shows load–displacement curves at 4 K for the SUS304 specimens precracked at the RT. The maximum load increased with increasing magnetic field. The measurements of the crack length and related parameters are performed on these specimens. As defined in JIS Z 2284, the difference between the final crack extension, Δa_f, predicted by elastic compliance at the last unloading and the average physical crack extension, Δa_p, does not exceed $0.15 \Delta a_p$, and none of the nine physical measurements, a_{pi}, differ by more 7% from the average physical crack length, a_p. The crack length requirement can not be satisfied in the 0.2TCT specimens.

Figure 3 shows the *J*-resistance (*J–R*) curves at 4 K for the specimens precracked at RT. A quantitative measure of J_Q (candidate value of J_{Ic}) is operationally defined as the point of intersection of the power-law regression line

and a blunting line, $J = 2\sigma_Y \Delta a$, drawn at a 0.2 mm offset (σ_Y in the effective yield strength). The J_Q value of 58.6 kJ/m^2 at 6 T is higher than the J_Q value at 0 T (45.9 kJ/m^2).
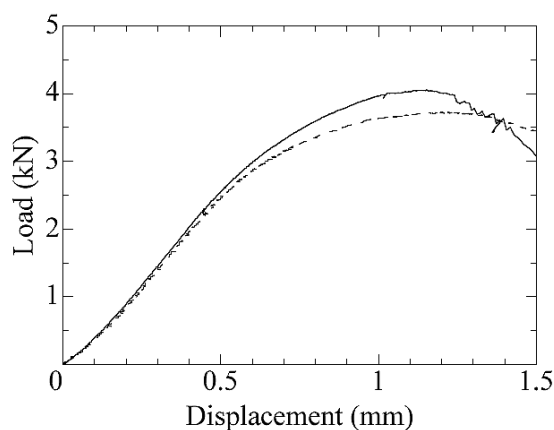
Fig. 2. Load–displacement curves for SUS304 CT specimens at 4 K (precracked at RT).
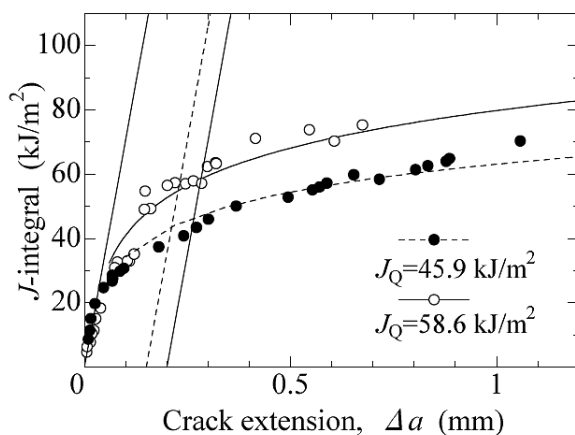
Fig. 3. *J–R* curves for SUS304 CT specimens precracked at 4 K (precracked at RT).

Figure 4 shows load–displacement curves at 4 K for the SUS304 specimens precracked at 77 K. The maximum load decreased with increasing magnetic field, in contrast to the specimens precracked at RT. Also, a small but sudden drop occurred under 6 T. This drop attributed to a pop-in crack growth. Measured crack extension data for the specimens precracked at 77 K show that the crack length requirement can not be satisfied.

Figure 5 shows the *J–R* curves at 4 K for the specimens precracked at 77 K. The J_Q value of 38.5 kJ/m^2 at 6 T is lower than the J_Q value at 0 T (42.6 kJ/m^2).

Changes in the fracture toughness are detected with an applied magnetic field, depending on the precracking temperature. A reduction in the J_Q value of the specimens precracked at 77 K with 6 T is due to the enhancement of martensitic transformation around the crack tip during the precracking stage. Figure 6 shows representative fractographic features of the fracture surfaces of the broken specimens

under 6 T precracked at RT and 77 K. Some brittle facets, assumed to be intergranular, were observed in the samples precracked at 77 K. It was implied that the higher brittleness of the specimens precracked at 77 K associated with high ferrite content, relative to the specimens precracked at RT.
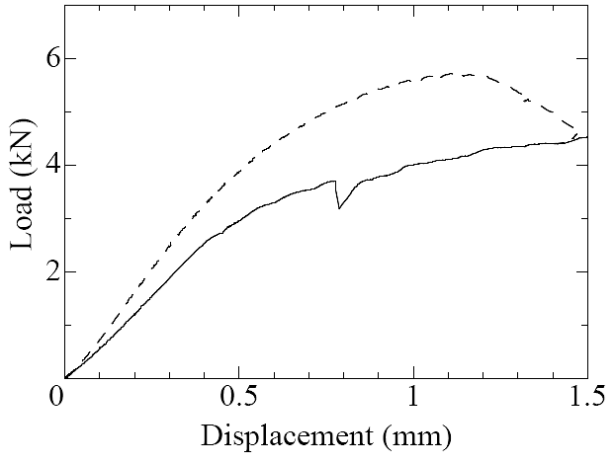
Fig. 4. Load–displacement curves for SUS304 CT specimens at 4 K (precracked at 77 K).
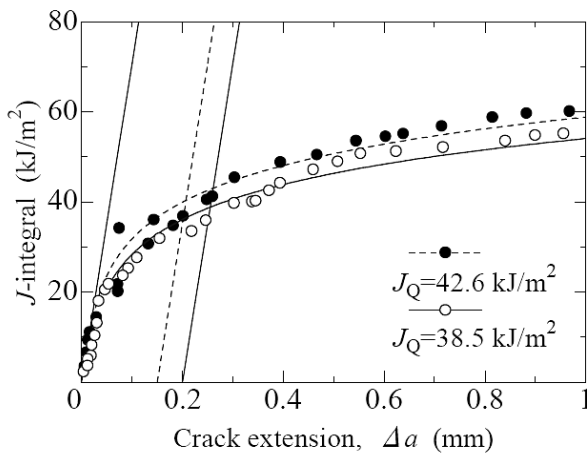
Fig. 5. *J–R* curves for SUS304 CT specimens precracked at 77 K.

Conclusions. The cryogenic fracture behavior of metastable austenitic stainless steel in magnetic field is characterized by elastic-plastic fracture toughness tests using CT specimens. It is found that magnetic field has negligible effect on the cryogenic tensile properties of SUS304 stainless steel. Also, magnetic field dependence of the cryogenic fracture toughness changes with the precracking temperature. For example, SUS304 stainless steel precracked at RT shows an increase in the fracture toughness at 4 K with the application of magnetic field. For SUS304 precracked at 77 K, magnetic field decreases the fracture toughness at 4 K. From the present study, it is expected to encourage further research on the fracture and fatigue of austenitic stainless steel in cryogenic high magnetic field environments.
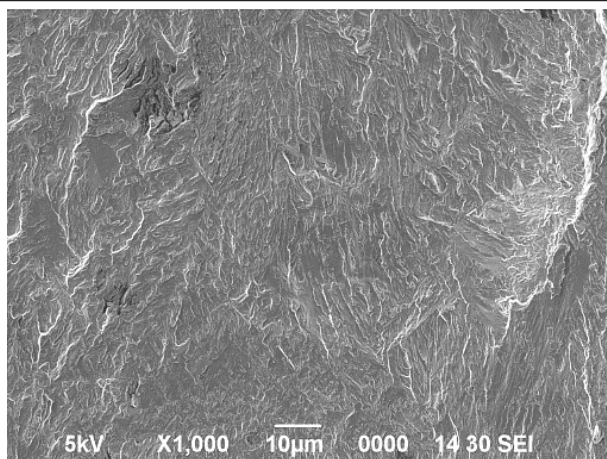
a
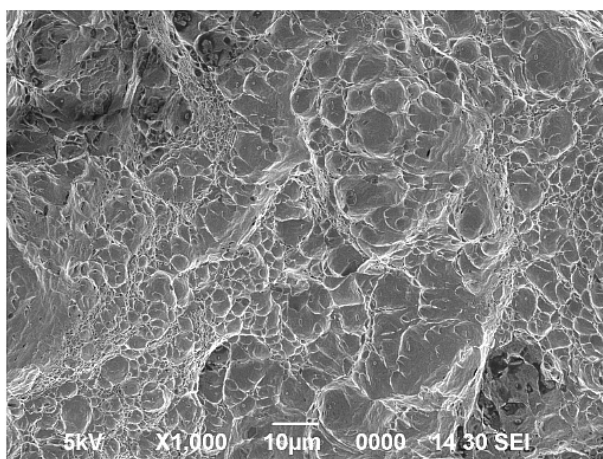
b

Fig. 6. Fractographs of broken specimens in 6 T precracked at RT (*a*) and 77 K (*b*).

Р е з ю м е

Досліджується вплив магнітного поля на закономірності руйнування мета-
стабільної аустенітної нержавіючої сталі за криогенних температур. При ви-
пробуванні компактних зразків на розтяг у середовищі рідкого гелію при
температурі 4 К за наявності і відсутності магнітного поля отримано експери-
ментальні значення пружно-пластичної в'язкості руйнування та проаналізо-
вано вплив магнітного поля на ці параметри. За допомогою магнітного
методу виконано кількісний фазовий аналіз. Поверхні руйнування досліджу-
вали на скануючому мікроскопі з метою оцінки кореляції отриманих пара-
метрів руйнування.

1. J. W. Chan, J. Glazer, Z. Mei, et al., "Fracture toughness of 304 stainless steel
   in an 8 tesla field," *Acta Metall. Mater.*, **38**, 479–487 (1990).

2. E. Fukushima, S. Kobatake, M. Tanaka, and H. Ogiwara, "Fracture toughness tests on 304 stainless steel in high magnetic fields at cryogenic temperatures," *Adv. Cryo. Eng.*, **34**, 367–370 (1988).

3. S. Murase, S. Kobatake, M. Tanaka, et al., "Effects of a high magnetic field on fracture toughness at 4.2 K for austenitic stainless steels," *Fusion Eng. Des.*, **20**, 451–454 (1993).

4. J. W. Chan, D. Chu, A. J. Sunwoo, and J. W. Morris, Jr., "Metastable austenites in cryogenic high magnetic field environments," *Adv. Cryo. Eng.*, **38**, 55–59 (1992).

5. Y. Yamaguchi, K. Horiguchi, Y. Shindo, et al., "Fracture and deformation properties of Ni–Fe superalloy in cryogenic high magnetic field environments," *Cryogenics*, **43**, 469–475 (2003).

6. Y. Shindo, Y. Yamaguchi, and K. Horiguchi, "Small punch testing for determining the cryogenic fracture properties of 304 and 316 austenitic stainless steels in a high magnetic field," *Cryogenics*, **44**, 789–792 (2004).

7. *JIS Z 2284. Method of Elastic-Plastic Fracture Toughness J_{Ic} Testing for Metallic Materials in Liquid Helium*, Japanese Standards Association (1998).

8. Y. Shindo, K. Horiguchi, and J. Yamada, "Specimen size effects in the cryogenic fracture toughness testing of Fe–12Cr–12Ni–10Mn–0.24N stainless steel," *Fusion Eng. Des.*, **73**, 1–7 (2005).

9. *ISO 19819. Metallic Materials – Tensile Testing in Liquid Helium*, International Organization for Standardization (2004).